

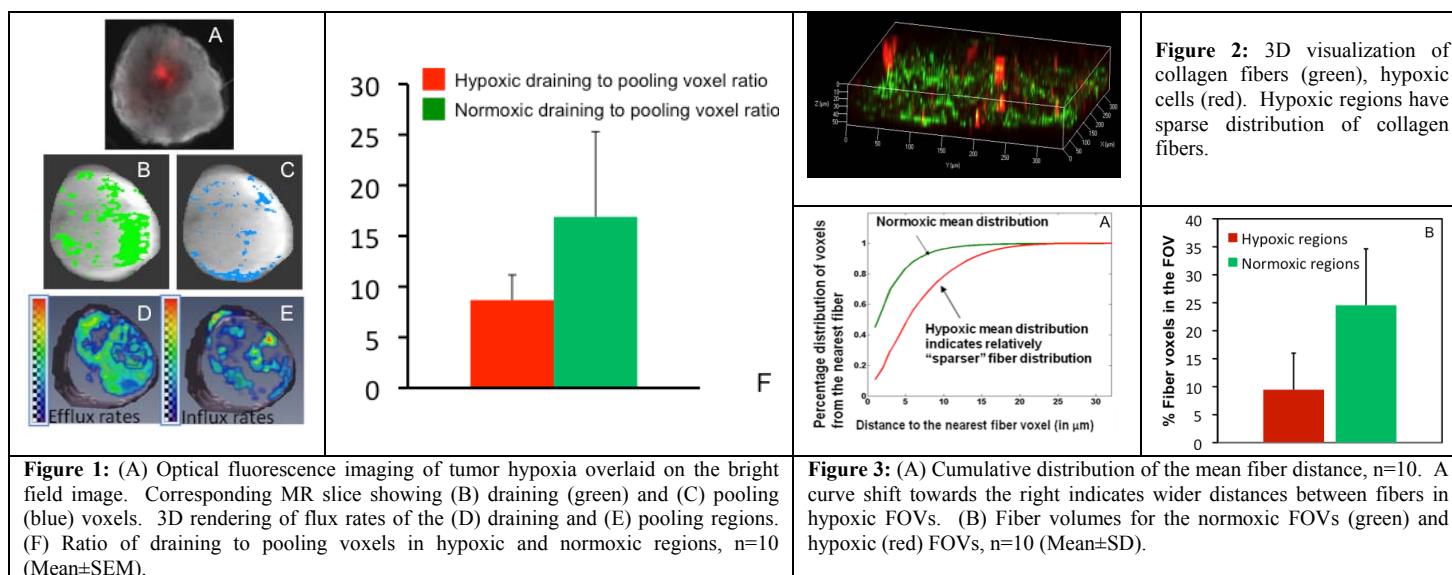
Characterization of macromolecular transport in hypoxic tumor environments with disrupted collagen I fibers

S. M. Kakkad¹, M-F. Penet¹, A. Pathak¹, M. Solaiyappan¹, V. Raman¹, K. Glunde¹, and Z. M. Bhujwala¹

¹JHU ICMIC Program, Russell H. Morgan Department of Radiology and Radiological Science, Johns Hopkins University School of Medicine, Baltimore, MD, United States

Introduction: Tumors display abnormal physiological environments such as hypoxia [1], which primarily arises from their abnormal and chaotic vasculature. Since the discovery of the hypoxia inducible factor (HIF) and the presence of hypoxia response elements (HREs) as transcriptional controls in multiple genes [2], it is becoming increasingly evident that the physiological environment and hypoxia in particular, plays an important role in the cancer phenotype. Hypoxia is associated with increased resistance to radiation and chemotherapy, and a more aggressive phenotype. Our purpose here was to investigate the role of hypoxia in altering collagen I fibers in the extracellular matrix (ECM), and its effect on macromolecular fluid transport. To study the relationship between hypoxia, macromolecular fluid transport, and collagen I fiber distribution, we have combined MRI of the macromolecular contrast agent (MMCA) albumin-GdDTPA, to detect interstitial fluid transport, with second harmonic generation (SHG) microscopy, to measure collagen fibers distribution. SHG microscopy is a nonlinear optical process in which noncentrosymmetric molecular structures, such as collagen I fibers generate a signal at half of the incident light's wavelength. SHG microscopy can therefore be used to image collagen I fibers [3]. These studies were performed in the MDA-MB-231 human breast cancer xenograft model genetically engineered to express tdTomato red fluorescent protein (RFP) under hypoxic conditions.

Methods: Female SCID mice were inoculated in the upper right thoracic mammary fat pad with 2×10^6 MDA-MB-231 cells stably expressing tdTomato RFP under control of the HRE of VEGF [4]. Imaging was performed once tumor volumes were approximately 400-500 mm³. Interstitial transport parameters were measured from quantitative T₁ maps obtained before and following intravenous administration of the contrast agent albumin-GdDTPA (500 mg/kg dose) on a 4.7T Bruker spectrometer. Images were acquired in two "phases" corresponding to the biphasic kinetics of the MMCA. The "early phase" images obtained over the initial 30 min were used to characterize vasculature. Since drainage of macromolecules in and around tumors either by convection or by the lymphatics is a slow event, the second block of MR data was acquired up to 140 min post contrast and was used to characterize interstitial transport. Interstitial parameters derived included number of draining and pooling voxels, draining and pooling rates, and volumes as previously described [5]. Following MRI, optical imaging of fresh tissue slices corresponding to the MR-imaged slices was performed to characterize interstitial transport in hypoxic regions. The tumor was immobilized in the coil using agar gel for accurate colocalization between MRI and the optical images of fresh tissue slices. These optical images, acquired with a 1x objective, were used to map the MRI data to hypoxic and normoxic regions on the slices. SHG microscopy of these slices was performed using a 25x lens on a Zeiss 710 LSM NLO confocal microscope system equipped with a 680-1080 nm tunable Coherent Chameleon Vision II laser with automated pre-compensation and extremely fast scanning at 40 nm/s. 3D image stacks were acquired from various fields of view (FOVs) in the hypoxic and normoxic regions. The fluorescence from RFP expressing hypoxic cells was imaged with excitation wavelength 543 nm, detected at 570-620 nm. Collagen I fibers were imaged from the same FOV using SHG microscopy with incident laser light of 880 nm, detected at 410-470 nm. Collagen I fiber distribution was visualized and characterized in the hypoxic and normoxic regions using an in-house 3D analysis software developed to quantify fiber distance distributions and volumes. We computed the 3D Euclidian distance maps and used their frequency distributions to characterize the porosity of the collagen fiber distribution in hypoxic and normoxic regions. Fiber volume was also computed for these FOVs.



Results: We were able to correlate the oxygenation from the optical image (Figure 1A) to the transport parameters from the MRI data (Figure 1B, C). Our preliminary studies revealed increased drainage in normoxic regions compared to hypoxic regions (Figures 1B and C). Figures 1D and 1E show the 3D representative efflux and influx rates. There was a trend towards higher drainage to pooling voxel ratio in normoxic regions compared to hypoxic regions as shown in Figure 1F ($p = 0.18$). A representative SHG image of the collagen I fiber distribution is shown in Figure 2. Quantification of collagen I fiber distribution and volume from several FOVs is shown in Figure 3A and 3B, respectively. SHG-detected collagen I fiber characterization of tumor slices revealed significantly lower fiber density ($p=0.0149$) and volume ($p=0.0008$) in hypoxic regions.

Discussion: Here, for the first time, we have combined MRI with SHG microscopy to relate differences in collagen I fibers between hypoxic and normoxic tumor regions to macromolecular fluid transport. A higher number of MMCA draining voxels were observed in normoxic regions which also exhibited a denser mesh of collagen fibers. In contrast, there were fewer draining voxels in hypoxic regions which also exhibited fewer and structurally altered collagen fibers. These data suggest that hypoxic areas are 'silent' zones with very little movement of MMCA as detected by this method.

References: 1. Hofbauer, K. H. *et al.*, Eur J Biochem, 2003; 2. Semenza, G. L. Biochem Pharmacol, 2000; 3. Schenke-Layland, K. *et al.*, Adv Drug Deliv Rev, 2006; 4. Raman *et al.*, Cancer Research, 2006; 5. Pathak *et al.*, Cancer Research, 2006.

Acknowledgement: This work was supported by NIH P50 CA103175 and P30 CA006973. We thank Mr. Gary Cromwell for technical assistance.